ACS SyntheticBiology

pubs.acs.org/synthbio Technical Note

A Standardized Inverter Package Borne by Broad Host Range Plasmids for Genetic Circuit Design in Gram-Negative Bacteria

Huseyin Tas, Ángel Goñi-Moreno, and Víctor de Lorenzo*

Cite This: https://dx.doi.org/10.1021/acssynbio.0c00529 Read Online

ACCESS | Metrics & More | Article Recommendations | Supporting Information

ABSTRACT: Genetically encoded logic gates, especially inverters—NOT gates—are the building blocks for designing circuits, engineering biosensors, or decision-making devices in synthetic biology. However, the repertoire of inverters readily available for different species is rather limited. In this work, a large whole of NOT gates that was shown to function previously in a specific strain of *Escherichia coli*, was recreated as broad host range (BHR) collection of constructs assembled in low, medium, and high copy number plasmid backbones of the SEVA (Standard European Vector Architecture) collection. The input/output function of each of the gates was characterized and parametrized in the environmental bacterium and metabolic engineering chassis *Pseudomonas putida*. Comparisons of the resulting fluorescence cytometry data with those published for the same gates in *Escherichia coli* provided useful hints on the portability of the corresponding gates. The hereby described inverter package (20 different versions of 12 distinct gates) borne by BHR plasmids thus becomes a toolbox of choice for designing genetic circuitries in a variety of Gram-negative species other than *E. coli*.

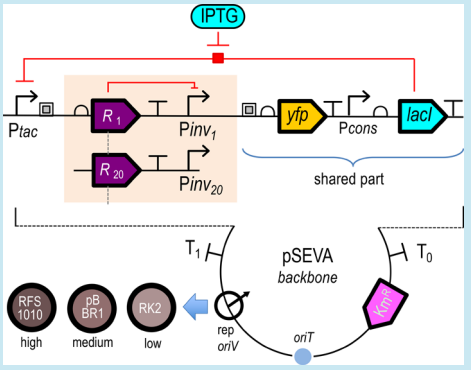

KEYWORDS: *broad host range tools, inverter library, gates, Pseudomonas putida, flow cytometry, biosensor, automated circuit design*

The design and implementation of genetic circuits is one of trademarks of contemporary synthetic biology.[1] The archetypal approach involves abstracting biological cues (e.g., effectors, metabolites, proteins) and physicochemical signals (e.g., inducers, temperature) as inputs. These are processed through a more or less complex computation layer (most often assembled with regulatory parts: transcriptional factors, riboregulators, *etc.*) which then releases another biological signal as the output. This in turn can be used as the input for another node of the circuit and so on.[2,3] Further abstraction of biological circuits as wholes of Boolean logic gates enables a superior level of complexity, as shown by a suite of examples involving rewiring of stress responses, detection of environmental contaminants, implementation of cellular calculators, and others.[4−7] Yet, as the demand for increasingly complex circuits grows,[5,8,9] so does the interest in automation of their design and execution. One major landmark in this direction was the publication in 2016 of the CelloCAD platform,[5] a complete operative system for virtual assembly and eventual implementation of logic circuits in *E. coli* through a combination of series of NOR gates—based themselves on a large collection of well characterized promoter/repressor pairs (i.e., inverters or NOT gates). This tool affords automated design and simulation in seconds of complex genetic networks with successful prediction of >70% of all states shown by the actual DNA constructs once synthesized and knocked in *E. coli*.[5,7] Yet, due to the material nature of the building blocks, CAD tools such as Cello are inherently restrictive to single strains or species. While these systems may work well in a given organism, the parameters and general behavior can change very significantly when passed to other hosts. This is a considerable issue when circuits are desired to compute signals under environmental and industrial conditions for which *E. coli* is not an optimal chassis.

On this basis we set out to engineer a robust and easy-to-use package of standardized NOT gates that could be used for circuit design in Gram-negative bacteria other than *E. coli* and that—once characterized in the host of interest—could benefit from the CelloCAD software[5] for automatic assembly of the cognate DNA.

To this end, we recreated the DNA sequence encoding each of the inverters available in the Cello platform and pass them to vectors of the broad host range SEVA (Standard European Vector Architecture[10]) collection with low, medium, and high copy numbers. The general organization of the constructs is sketched in Figure 1. These inverters are based on the transcriptional inhibition exerted by given repressors expressed under the control of IPTG on target promoters. Note that the

Received: October 18, 2020

https://dx.doi.org/10.1021/acssynbio.0c00529
ACS Synth. Biol. XXXX, XXX, XXX−XXX

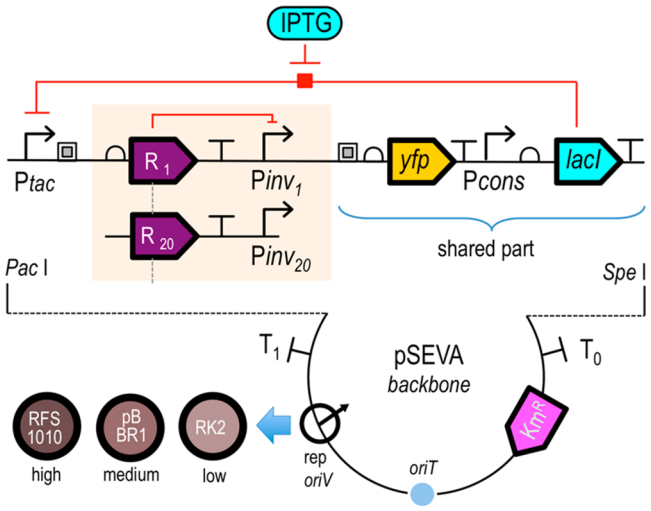

Figure 1. Schematic representation of genetically encoded inverters assembled in BHR plasmids. The organization of 20 variants of functional parts assembled following the SEVA standard is sketched (components not to scale). Similarly to the earlier collection for *E. coli*[5] there are segments shared by all constructs, that is, the P*tac/lacI*/IPTG-dependent expression system for each of the repressor/SD (Shine-Dalgarno sequence) combinations (R_1 to R_{20}) and the *yfp* gene used for fluorescent readout of inverter performance. Segments coming from SEVA backbone (T_1 and T_0 terminators, origin of conjugal transfer *oriT*) and the Km resistance gene are common to all constructs as well. The variable parts include [i] the DNA encoding the SD, the repressor gene (R) and the cognate repressible promoter (P*inv*) upstream of the reporter *yfp* and [ii] the BHR origin of replication: RK2, pBBR1 or RSF1010, each of them supporting a different copy numbers as indicated.

specific functional DNA borne by each plasmid is flanked by upstream and downstream terminators added by the SEVA structure to mitigate potential readthrough from vector promoters. The plasmids backbones were retrieved from the SEVA database and repository.[10]

In practical terms, each of the segments encoding the gates was amplified from the collection of *E. coli* NEB10*β* strains bearing p15A/Km^R vectors (~15 copies) inserted with the cognate DNA.[5] Primers (Merck Sigma-Aldrich, Inc.) were designed for adding SEVA-compatible PacI and SpeI restriction sites to the extremes of the amplicons generated with the Q5 High-Fidelity DNA polymerase (New England BioLabs, Inc.). The oligonucleotides used for amplification of the DNA of the NOT gates and verification of the constructs are listed in Supplementary Table S2. Following PCR, the resulting fragments where separately cloned in pSEVA221 (RK2*oriV*, ≤5 copies/cell), pSEVA231 (BBR1*oriV*, ~30 copies), and pSEVA251 (RFS1010*oriV*, ≥50 copies) and first captured, verified, and resequenced in the host strain *P. putida* KT2440. The complete catalogue of constructs is listed in Table 1.

Note that some gates (those designated BM3R1-B1, PhlF-P3, QacR-Q2, SrpR-S2, and SrpR-S3) could not be cloned in the higher copy number vectors, presumably due to the toxicity effects of the encoded repressor proteins. The collection (Table 1 and Supplementary Table S1) includes a total of 12 inverters, some of them bearing two or more variants of the Shine-Dalgarno sequence of the repressor gene that changes its expression levels. For example, AmeR-F1 (AmeR is the gate and F1 is the Shine-Dalgarno sequence) has only one version

Table 1. Library of Available Genetically-Encoded Inverters and Auxiliary Plasmids in SEVA Vectors with Three Available Copy Numbers[a]

Inverters	Low Copy Number	Medium Copy Number	High Copy Number
AmeR-F1	✓	✓	✓
AmtR-A1	✓	✓	✓
BetI-E1	✓	✓	✓
BM3R1-B1	✓	✓	-
BM3R1-B2	✓	✓	✓
BM3R1-B3	✓	✓	✓
HlyIIR-H1	✓	✓	✓
IcaRA-I1	✓	✓	✓
LitR-L1	✓	✓	✓
LmrA-N1	✓	✓	✓
PhlF-P1	✓	✓	✓
PhlF-P2	✓	✓	✓
PhlF-P3	✓	✓	-
PsrA-R1	✓	✓	✓
QacR-Q1	✓	✓	✓
QacR-Q2	✓	✓	-
SrpR-S1	✓	✓	✓
SrpR-S2	✓	✓	-
SrpR-S3	✓	✓	-
SrpR-S4	✓	✓	✓
Auto-fluorescence	✓	✓	✓
Standardization	✓	✓	✓
Promoter Activity	✓	✓	✓

[a]See Supplementary Table S1 for plasmid names and cargoes. The repressor borne by each of the gates is described in ref 5. Availability of the constructs is ticked with a check mark in each case. The complete DNA sequences are listed in Supplementary Data S3. Unattainable plasmids—surely due to excessive copy number—are marked with (−).

of the ribosomal binding site of the repressor gene; however, SrpR has four versions (SrpR-S1, SrpR-S2, SrpR-S3, SrpR-S4 (SrpR is the gate and S1, S2, S3, and S4 are the four different SDs). Note also that the arrangement of functional parts of the gates in the SEVA vectors is identical to the one originally adopted in the p15A/Km^R vectors of the Cello platform (Figure 1). In addition to the plasmids bearing 20 inverters, we built a set of reference constructs allowing relative promoter units (RPU) to be converted and compared between different conditions (see below). These references (Supplementary Figure S1) include [i] autofluorescence plasmids (recreating the functional parts of pAN1201[5] and consisting of each of the backbone plasmids but without any insert, for example, missing the repressor/target promoter segments highlighted in Figure 1, [ii] RPU standard plasmids derived from pAN1717[5] in which *yfp* is expressed through the constitutive promoter J23101 and which are used in combination with the autofluorescence plasmid for converting YFP readouts of each inverter into RPU (see eq 1 below) and [iii] promoter activity plasmid recreating pAN1818,[5] which is used for measuring the promoter activity (pTac-YFP) based on inducer concentrations (Supplementary Figure S1).

The library of constructs listed in Table 1 and Supplementary Table S1 is expected to ease utilization of CelloCAD as a genetic programming tool in a suite of Gram-negative bacteria. Note that users have a choice to pick the same gate borne by plasmids with different copy numbers, what may be critical to avoid potential toxicity. Adoption of the standard SEVA format gives two additional advantages. While the construct library of Supplementary Table S1 was built on vectors with a Km resistance gene, the modularity of the SEVA format makes its replacement by an alternative antibiotic marker for selection[10,11] easy. Also, the BHR nature of the

https://dx.doi.org/10.1021/acssynbio.0c00529
ACS Synth. Biol. XXXX, XXX, XXX−XXX

standardized constructs affords their implantation in diverse Gram-negative hosts, thereby giving a chance to compare their performance in different species and thus learn about interoperability and context dependencies in circuit designs.

To validate these features we tested and parametrized the whole low-copy number versions of the inverter library of Supplementary Table S1 in the environmental bacterium and synthetic biology chassis *Pseudomonas putida* KT2440.[12,13] The experimental workflow to this end (Figure 2) was designed

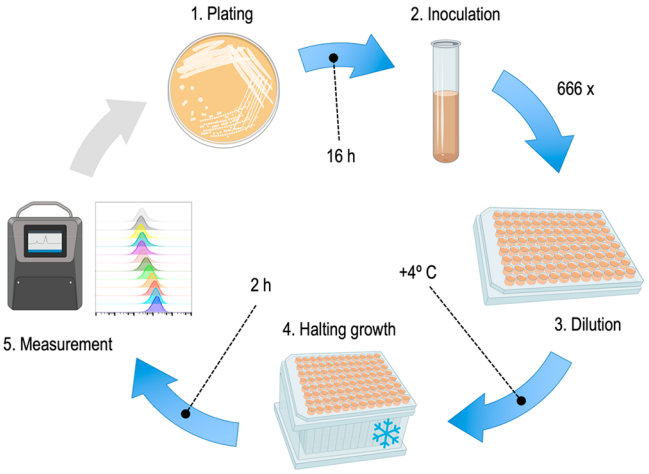

Figure 2. Experimental protocol used for performance measurement of the genetic inverters listed in Table 1 in *P. putida* KT2440. In all experiments bacteria were grown in M9 medium adapted for growth of *P. putida* (250 mL of liquid culture containing 25 mL × 10 M9 salts, 500 μL of 1 M $MgSO_4$, 2.2 mL of 20% citrate, and milli-Q H_2O to volume; 50 μg mL^{-1} kanamycin was added to secure plasmid retention (all of them Km^R)). For the experiments, saturated overnight cultures were diluted >600-fold in the wells of a microtiter plate with 200 μL per well, added with IPTG concentrations ranging 0 to 1000 μM and incubated at 30 °C with shaking for 24 h. Cultures (typically reaching OD_{600} ~0.2−0.3) were then kept in the cold for the rest of the procedure. YFP fluorescence distribution of each sample was measured with a Miltenyi Biotec MACS flow cytometer at channel B1 with an excitation of 488 nm and emission of 525/50 nm. For each sample 30 thousand events were collected with singlet gating. Calibration was done by using MACSQuant Calibration Beads (see text for explanation). Figure composed with images from https://biorender.com/ (subscription 89B77366-0004).

considering the specific needs of *P. putida* for growth as detailed in the legend of the figure. Once strains bearing each of the constructs were generated, transformants were grown and IPTG concentrations of (5−1000 μM) added to activate each of the devices, for a total 24 h period. YFP fluorescence emission detected with a flow cytometer was recorded after 24 of IPTG addition. Data were then analyzed with FlowJo software (https://www.flowjo.com/). An important detail was that the autogating option of the software was set considering at least 50% of the events covered while Forward and Side scatters were plotted. The same gating conditions were applied to all specimens in the same group and repeated for all the samples.

On the basis of the thereby produced data we quantified the output of the individual devices at each condition as standard RPUs (relative promoter units). This was done by characterizing the fluorescence values emitted by the bacterial population of the cultures exposed to IPTG levels covering an induction ranges from none to saturation (in our case 12 points of growing effector concentrations). The RPU value at each point can then be calculated with eq 1:

$$\mathrm{RPU} = \frac{\langle \mathrm{YFP} \rangle - \langle \mathrm{YFP} \rangle_{\mathrm{autofluorescence}}}{\langle \mathrm{YFP} \rangle_{\mathrm{standardization}} - \langle \mathrm{YFP} \rangle_{\mathrm{autofluorescence}}} \quad (1)$$

Where ⟨YPF⟩ is the median fluorescence value from the gate of interest that is to be converted into RPU (from either the inverter-bearing plasmids or the control promoter activity plasmid), $\langle \mathrm{YPF} \rangle_{\mathrm{autofluorescence}}$ is the median fluorescence value of autofluorescence plasmid, $\langle \mathrm{YPF} \rangle_{\mathrm{standardization}}$ is the median fluorescence value from the standardization plasmid. Next, the output versus input values of each inverter were represented in a response function plot generated with Hill fits and utilizing the RPU figures as the input to the calculations. Specifically, Hill equation parameters were estimated by plotting each inducer levels with their corresponding standardized median fluorescence values that were experimentally obtained for this study (Supplementary Data S2) by means of eq 2:

$$y = y_{\mathrm{min}} + \frac{(y_{\mathrm{max}} - y_{\mathrm{min}})k^n}{k^n + x^n} \quad (2)$$

where y is the output promoter activity, y_{min} is the minimum observed value for promoter activity, y_{max} is the maximum observed value for promoter activity, k is the input value for which half-maximum value for output promoter is reached, and n is the Hill coefficient.

Experimental response data were thus entered in the above Hill equation. The corresponding Hill parameters are provided in Supplementary Table S3 for both *E. coli* (retrieved from www.cellocad.org) and *P. putida* values (this study). Fitting was performed with MATLAB using the scripts provided in Supplementary Data S1. The resulting characterization of the 20 inverters (listed in the Supplementary Table S1) in *P. putida* based on the protocols and calculations above is summarized in Figure 3. The data showed a range of both divergences and similarities in the behavior of the inverters in

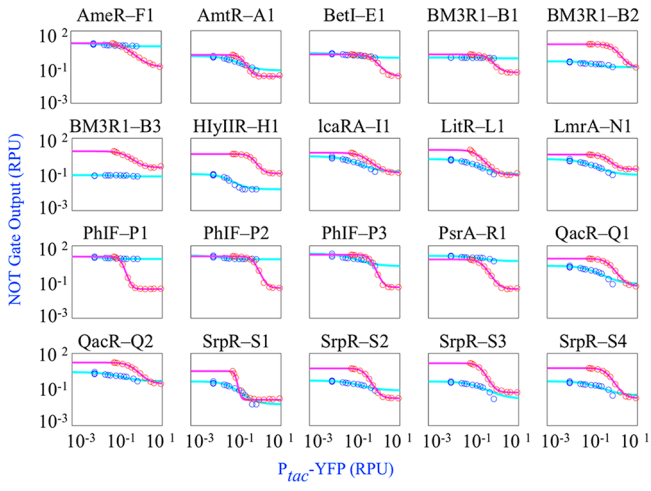

Figure 3. Behavior of genetically encoded inverters in *P. putida* vs *E. coli*. The panel shows the comparisons of the Hill fits of the same inverters in *E. coli* NEB10β (magenta; data retrieved from ref 5) and their behavior in *P. putida* KT2440 (cyan; experimental from this study). The *X*-axes correspond to the activity of the IPTG-inducible pTac promoter, and the *Y*-axes indicate the activity of corresponding inverters. Both axes indicate YFP expression in RPUs.

https://dx.doi.org/10.1021/acssynbio.0c00529
ACS Synth. Biol. XXXX, XXX, XXX−XXX

either host. Despite an expected change in readout values and dynamic ranges, six devices (SrpR-S1, AmtR-A1, LitR-L1, PhIF-P3, QacR-Q2, HIyIIR-H1) had patterns qualitatively comparable to the response curves and the ON/OFF states described for *E. coli*. Based on the observed input/output patterns, such inverters showed the required parameter compatibility and therefore they are eligible as first or second position gate for circuit design in *P. putida* following the Cello criterium.[5] Yet for other series of devices (i.e., AmeR-F1, BetI-E1, BM3R1s, PhIFs, PsrA-R1, and SrpR-S2) there was little if any similarity in their input/output transfer functions when placed in either host. Furthermore, their ON/OFF states were not different enough, thereby curbing any possible compatibility for assembling logic circuitry with two or more of these gates.

While these data expose the limitations of just exporting genetic devices from one species to the other, the large repertoire of inverters also enable users to pick the ones the parameters of which are compatible with the CelloCAD tool for automation of circuit designs[5] in specific Gram-negative hosts different of *E. coli* or *P. putida*. Furthermore, the data set associated with Figure 3 encrypts valuable, quantitative information on the interoperability of parts and circuits between different biological recipients of the same constructs, an issue hardly tackled thus far in the Synthetic Biology literature[14−16]

In sum, we believe that the hereby described collection of inverters available in a BHR format will help to expand the possibilities of genetic programming toward bacteria other than *E. coli* but still be interesting from a SynBio-inspired biotechnological perspective. Furthermore, their testing and parametrization in various hosts may deliver general portability rules that thus far rely on a mere trial-and-error exercise. The whole collection of constructs is available through the SEVA database and vector repository at http://seva.cnb.csic.es.

■ ASSOCIATED CONTENT

Supporting Information

The Supporting Information is available free of charge at https://pubs.acs.org/doi/10.1021/acssynbio.0c00529.

Supplementary Figure S1 (PDF)
Supplementary Table S1: BHR Inverters (XLSX)
Supplementary Table S2: Primers (XLSX)
Supplementary Table S3: Insulated gate response functions (XLSX)
Supplementary Data S1: Scripts (ZIP)
Supplementary Data S2: Median Values (XLSX)
Supplementary Data S3: Plasmid Maps (ZIP)

■ AUTHOR INFORMATION

Corresponding Author

Víctor de Lorenzo − *Systems Biology Department, Centro Nacional de Biotecnología-CSIC, Madrid 28049, Spain;* orcid.org/0000-0002-6041-2731; Phone: 34- 91 585 45 36; Email: vdlorenzo@cnb.csic.es; Fax: 34- 91 585 45 06

Authors

Huseyin Tas − *Systems Biology Department, Centro Nacional de Biotecnología-CSIC, Madrid 28049, Spain;* orcid.org/0000-0003-4804-2237

Ángel Goñi-Moreno − *School of Computing, Newcastle University, Newcastle Upon Tyne NE4 5TG, U.K.; Instituto Nacional de Investigación y Tecnología Agraria y Alimentaria (INIA), Centro de Biotecnología y Genómica de Plantas (CBGP, UPM-INIA), Universidad Politécnica de Madrid (UPM), Pozuelo de Alarcón, Madrid 28223, Spain*

Complete contact information is available at: https://pubs.acs.org/10.1021/acssynbio.0c00529

Author Contributions

H.T., A.G.-M., and V.d.L. planned the experiments, analyzed and discussed the data, and contributed to the writing of the article.

Funding

This work was funded by the SETH Project of the Spanish Ministry of Science RTI 2018-095584-B-C42, the MADONNA (H2020-FET-OPEN-RIA-2017-1-766975), BioRoboost (H2020-NMBP-BIO-CSA-2018), SYNBIO4FLAV (H2020-NMBP/0500) and MIX-UP (H2020-Grant 870294) Contracts of the European Union, the S2017/BMD-3691 InGEMICS-CM Project of the Comunidad de Madrid (European Structural and Investment Funds), and the SynBio3D project of the UK Engineering and Physical Sciences Research Council (EP/R019002/1). AG-M was also supported by grants from Comunidad de Madrid (Atracción de Talento Program, grant 2019-T1/BIO-14053) and the Severo Ochoa Program for Centres of Excellence in R&D from the Agencia Estatal de Investigación of Spain, grant SEV-2016-0672 (2017-2021).

Notes

The authors declare no competing financial interest.

■ ACKNOWLEDGMENTS

We are indebted to Chris Voigt and Alec Nielsen (MIT) for sharing the collection of NOT gates developed for the Cello platform.

■ ABBREVIATIONS

BHR, broad host range; SD, Shine-Dalgarno sequence; RBS, ribosomal binding sequence; IPTG, isopropyl thiogalactopyranoside; CAD, computer-assisted design; SEVA, Standard European Vector Architecture.

■ REFERENCES

(1) Slusarczyk, A. L., Lin, A., and Weiss, R. (2012) Foundations for the design and implementation of synthetic genetic circuits. *Nat. Rev. Genet. 13*, 406−420.

(2) Bashor, C. J., and Collins, J. J. (2018) Understanding biological regulation through synthetic biology. *Annu. Rev. Biophys. 47*, 399−423.

(3) Moon, T. S., Lou, C., Tamsir, A., Stanton, B. C., and Voigt, C. (2012) Genetic programs constructed from layered logic gates in single cells. *Nature 491*, 249−253.

(4) Miyamoto, T., Razavi, S., DeRose, R., and Inoue, T. (2013) Synthesizing biomolecule-based Boolean logic gates. *ACS Synth. Biol. 2*, 72−82.

(5) Nielsen, A. A., Der, B. S., Shin, J., Vaidyanathan, P., Paralanov, V., Strychalski, E. A., Ross, D., Densmore, D., and Voigt, C. A. (2016) Genetic circuit design automation. *Science 352*, No. aac7341.

(6) Stanton, B. C., Nielsen, A. A., Tamsir, A., Clancy, K., Peterson, T., and Voigt, C. A. (2014) Genomic mining of prokaryotic repressors for orthogonal logic gates. *Nat. Chem. Biol. 10*, 99−105.

(7) Shin, J., Zhang, S., Der, B. S., Nielsen, A. A., and Voigt, C. A. (2020) Programming *Escherichia coli* to function as a digital display. *Mol. Syst. Biol. 16*, No. e9401.

(8) Mohammadi, P., Beerenwinkel, N., and Benenson, Y. (2017) Automated Design of Synthetic Cell Classifier Circuits Using a Two-Step Optimization Strategy. *Cell Syst 4*, 207−218.
(9) Xiang, Y., Dalchau, N., and Wang, B. (2018) Scaling up genetic circuit design for cellular computing: advances and prospects. *Nat. Comput. 17*, 833−853.
(10) Martinez-Garcia, E., Goni-Moreno, A., Bartley, B., McLaughlin, J., Sanchez-Sampedro, L., Pascual Del Pozo, H., Prieto Hernandez, C., Marletta, A. S., De Lucrezia, D., Sanchez-Fernandez, G., Fraile, S., and de Lorenzo, V. (2020) SEVA 3.0: an update of the Standard European Vector Architecture for enabling portability of genetic constructs among diverse bacterial hosts. *Nucleic Acids Res. 48*, D1164−D1170.
(11) Martinez-Garcia, E., Aparicio, T., Goni-Moreno, A., Fraile, S., and de Lorenzo, V. (2015) SEVA 2.0: an update of the Standard European Vector Architecture for de-/re-construction of bacterial functionalities. *Nucleic Acids Res. 43*, D1183−1189.
(12) Nikel, P. I., Martínez-García, E., and de Lorenzo, V. (2014) Biotechnological domestication of pseudomonads using synthetic biology. *Nat. Rev. Microbiol. 12*, 368−379.
(13) Martínez-García, E., and de Lorenzo, V. (2019) *Pseudomonas putida* in the quest of programmable chemistry. *Curr. Opin. Biotechnol. 59*, 111−121.
(14) Beal, J., Haddock-Angelli, T., Gershater, M., de Mora, K., Lizarazo, M., Hollenhorst, J., and Rettberg, R. (2016) Reproducibility of fluorescent expression from engineered biological constructs in *E. coli*,. *PLoS One 11*, No. e0150182.
(15) Khan, N., Yeung, E., Farris, Y., Fansler, S. J., and Bernstein, H. C. (2020) A broad-host-range event detector: expanding and quantifying performance between *Escherichia coli* and *Pseudomonas species*,. *Synth Biol. 5*, No. ysaa002.
(16) Boo, A., Ellis, T., and Stan, G.-B. (2019) Host-aware synthetic biology. *Curr. Op Syst. Biol. 14*, 66−72.

https://dx.doi.org/10.1021/acssynbio.0c00529
ACS Synth. Biol. XXXX, XXX, XXX−XXX